

Failure mechanism on sulfate attack and dissolved corrosion of diseased tunnel lining structure

Jinwang Mao¹, Ninghui Liang², Ru Yan³

¹College of Civil Engineering, Chongqing University, Chongqing, 400045, China

²National and Local Joint Engineering Research Center for Environmental Geological Disaster Prevention and Control in the Reservoir Area (Chongqing University), Chongqing, 400045, China

³Power China Chengdu Engineering Corporation Limited, Chengdu Sichuan, 610072, China

²Corresponding author

E-mail: ¹1003181257@qq.com, ²lning033@163.com, ³1271735867@qq.com

Received 11 July 2022; received in revised form 11 August 2022; accepted 22 August 2022
DOI <https://doi.org/10.21595/vp.2022.22869>



59th International Conference on Vibroengineering in Dubai, United Arab Emirates, October 22, 2022

Copyright © 2022 Jinwang Mao, et al. This is an open access article distributed under the Creative Commons Attribution License, which permits unrestricted use, distribution, and reproduction in any medium, provided the original work is properly cited.

Abstract. To study the corrosion failure mechanism of tunnel lining structure subjected to sulfate attack and dissolved corrosion, site investigation was carried out on a diseased tunnel in Chongqing. The corrosion products were analyzed by scanning electron microscopy (SEM), energy dispersive spectroscopy (EDS), X-ray diffraction (XRD) and Fourier transform infrared (FTIR) spectroscopy. The results showed that the tunnel lining structure had been exposed to groundwater containing substantial concentrations of salts (SO_4^{2-} , HCO_3^- , et al.) for many years, resulted that the concrete strength was lower than its design value. The formation of thaumasite made concrete lose its strength completely. Concrete structure would be destroyed when crystallization pressure exceeded the tensile strength of concrete. The tunnel also appeared dissolved corrosion which made the cement stone density and concrete strength reduce.

Keywords: diseased tunnel, site investigation, sulfate attack, dissolved corrosion, failure mechanism.

1. Introduction

Concrete sulfate attack is a complex process. Sulfate ions are transmitted to the interior of concrete to react with cement hydration products or crystallize out directly, causing the concrete to crack, peel off, even become soft crumbly degraded concrete and affect the lining structure strength and integrity [1].

It is necessary to reveal the mechanism of sulfate attack about tunnel lining structure and has achieved many meaningful results. In recent years, the research on the sulfate corrosion resistance of concrete structures become more and more in-depth. Ma et al. [2] presented the first case of thaumasite-related sulfate attack of field structures in China. For understanding the deterioration behavior of concrete. Ma et al. [3] found that the chemical corrosion of concrete lining was mainly caused by the formation of gypsum and thaumasite rather than the formation of ettringite. Yin et al. [4] studied the combined effect from sulfate and chloride on the corrosion in lining concretes through simulating the transport of corrosive ions in the solution. They found that the existence of chloride obviously decreased the corrosion of lining concrete under sulfate attack, and the depressing effect from chloride increased with the content of chloride in the chloride-sulfate composite solution. Different kinds of corrosion had occurred in engineering practice simultaneously. However, the engineering case of a tunnel which occurred sulfate attack and dissolved corrosion hadn't been reported.






In this paper, take a diseased tunnel in Chongqing as an example, the ion concentration in groundwater and the strength of secondary lining concrete were detected; the corrosion products were analyzed with SEM, EDS, XRD and FTIR, which is very representative to study tunnel sulfate attack mechanism.

2. Site investigation

The exposed and buried strata in the tunnel site area are mainly a set of neritic facies from the Lower Permian to the Mesozoic Jurassic Middle Shaximiao Formation and the sedimentary strata of carbonate rocks and clastic rocks in inland rivers and lakes. The severely corroded section of the tunnel crosses the strata consisting of purplish-red mudstone, gray-green argillaceous siltstone, thin-bedded sandstone, and marl of the Middle Triassic Badong Formation (T₂b). Two groups of fissures are mainly developed, with the angle between them is about 80°, presenting a state from slightly open to open.

Tunnel lining concrete suffered serious sulfate attack. The distribution of corrosion area was spreading from the construction joints of two adjacent molds. The lining surface was moist and appeared white crystallizations. Travertine could be seen where dripping water. There was a large area of concrete falling off within 1.5m above the arch foot and the soft crumbly degraded concrete could be seen at the arch foot. The site investigation results were shown in Table 1.

Table 1. Corrosion characteristics of tunnel lining concrete

1,8	1#	2#	3#	4#	5#
Character	The distribution of corrosion area	The soft crumbly degraded concrete	Travertine on the lining surface	Peeling of concrete on the tunnel lining	White crystallizations on the lining surface
Photos					

3. Experiment

3.1. Groundwater analysis

In order to analysis the salts concentration of groundwater. Water samples at the arch foot and initial support that suffered the most severe sulfate attack were collected. The ion chromatography instrument of Thermo Scientific (DIONEX AQUION RFIC) was used to analyze the ion concentration of the water samples.

3.2. Compression test

The rebound method and core sampling drilling were carried out to examine the concrete intensity and the degree of carbonization. Using LR-TH10 digital carbonization depth measuring instrument with 1 % phenolphthalein reagent to determine the concrete carbonation depth and ZC3-B rebound instrument was used to measure the concrete rebound strength. According to the relevant regulations of Technical Specification for Testing Concrete Strength with Drilling Core Method (JGJ/T 384-2016), the core samples ($d = 100$ mm) were processed into cylindrical specimens with a height-diameter ratio equal to 1. Then, a computer-controlled flexural compressive testing machine (YAW-300C) was used to test the concrete compressive strength.

3.3. SEM, EDS, XRD and FTIR analysis

In the site investigation process, samples of the soft crumbly degraded concrete, travertine and white crystals were carefully chosen and preserved for laboratory investigations. The samples preparation process of corrosion products is shown in Fig. 1. Firstly, the samples were placed in a dry crucible and put them in an oven at 50°C for 5 days. And then, the dried samples were grinded into powder by agate mortar. After grinding, passed through a sieve with an aperture of 0.074 mm

to obtain powder with a particle size no larger than 0.074 mm. Thus, samples used for SEM, EDS, XRD and FTIR had been prepared.

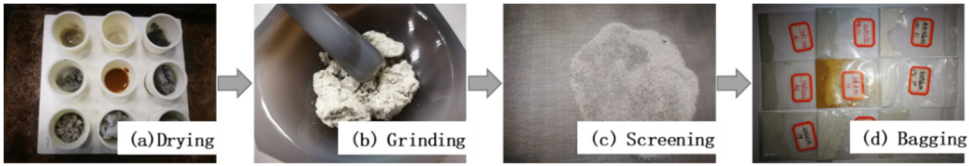


Fig. 1. Samples preparation process

4. Results and discussion

4.1. Ion concentration of groundwater

The salts concentrations of groundwater were shown in Table 2.

The results showed that the groundwater contains substantial concentrations of salts, especially sulfate ion. The SO_4^{2-} content of sample 3# reached 1180 mg/L. The HCO_3^- content of the groundwater was almost 100 mg/L-200 mg/L. The content of Mg^{2+} was relatively low and there was no Cl^- , Na^+ and K^+ basically. According to the environmental effects grade specified in Code for Durability Design of Concrete Structures in Highway Engineering (JTG/T 3310-2019), the tunnel was in medium-severe groundwater chemical corrosion environment and should be designed based on medium corrosion protection. Standard Standard for Design of Concrete Structure Durability (GB/T 50476-2019) ruled the strength grade of tunnel concrete should not be lower than C40 and corrosion resistant concrete needed to be applied, while the actual lining concrete was C25 ordinary concrete. It showed that the hydrogeological conditions were not ascertained accurately when the tunnel was constructed, which was one of the main reasons for the serious lining concrete corrosion.

Table 2. Ion concentration of groundwater samples

Sample	concentrations of salts (mg/L)						PH value
	SO_4^{2-}	Cl^-	Mg^{2+}	HCO_3^-	Na^+	K^+	
1#	828	3.47	48.6	157	12.1	2.16	7.18
2#	812	3.56	47.6	160	12.2	2.37	7.19
3#	1180	1.71	43.6	4.22	14	10.8	9.73

4.2. Concrete compressive strength

The compression test results of lining concrete cylinder specimens provided in Table 3.

From Table 3, we could see that only in individual locations, the compressive strength of concrete met its design requirements, the compressive strength of most specimens was lower than its design value basically, especially at K0+613, the strength was only 13.07 MPa, which was much lower than 25 MPa and reduced by about 50 %. It could be seen that the lining structure deteriorated seriously, and the safety grade of lining structure reduced greatly.

Table 3. Compressive strength of lining concrete cylinder specimen

Position (K0+)	500	520	541	560	578	598	613	638
Failure load (KN)	138.3	235.7	191.4	206.5	212.8	192.1	113.2	164.2
Compressive strength (MPa)	15.97	27.22	22.10	23.85	24.58	22.18	13.07	18.97

5. Sulfate attack mechanism

5.1. Thaumassite

The tunnel lining concrete suffered serious sulfate attack, especially at the arch foot, soft

crumbly degraded concrete was found in several places. The powder particle was used for SEM, XRD and FTIR analysis. Fig. 2 showed SEM images of the soft crumbly degraded concrete at two resolutions. It could be seen that there was little trace of the products of normal cement hydration such as calcium silicon hydrate (C-S-H) in the XRD trace due to the deterioration. Fig. 2(a) showed that a lot of club-shaped or needle crystals embedded irregularly in the pulpy material with large internal pores. And there was little CH crystal. Fig. 2(b) was the SEM image under higher magnification, showed that plenty of needle crystals up to 0.5 μm in diameter and 3-4 μm in length. It could be found the characteristics of crystal distribution was parallel orientation predominantly, and the surface was smooth. It was judged as ettringite or thaumasite preliminary.

The EDS spectrum of the soft crumbly degraded concrete was shown in Fig. 3. EDS analysis of O, S, Si and Ca indicated the presence of thaumasite. A higher Si and little Al peak indicated that these needle crystals were predominantly thaumasite and ettringite was almost absent. It could be preliminarily determined that the tunnel appeared thaumasite-type sulfate attack. But it was possible that the amorphous phase was closely associated with the thaumasite/ettringite crystals and interferes with the analytical results obtained by EDS.

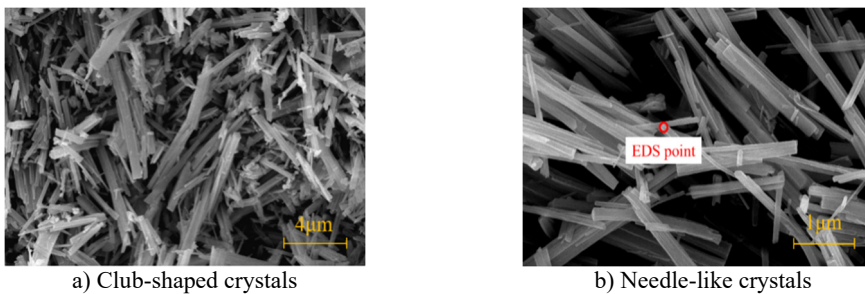


Fig. 2. SEM image of the soft crumbly degraded concrete

The XRD analysis result was shown in Fig. 4. It shown that several crystalline phases exist in the sample, including thaumasite, ettringite, gypsum and quartz. The characteristic peaks (0.956 nm, 0.551 nm, 0.467 nm, 0.387 nm, et al.) of thaumasite were similar to those of ettringite (0.972 nm, 0.561 nm, 0.486 nm, 0.387 nm, et al.) [5]. The diffraction peaks positions of thaumasite and ettringite were similar on the pattern, so it was difficult to identify them by XRD method.

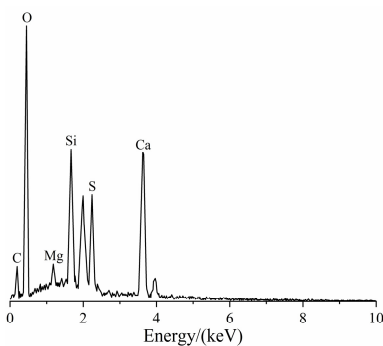


Fig. 3. EDS spectrum of the soft crumbly degraded concrete

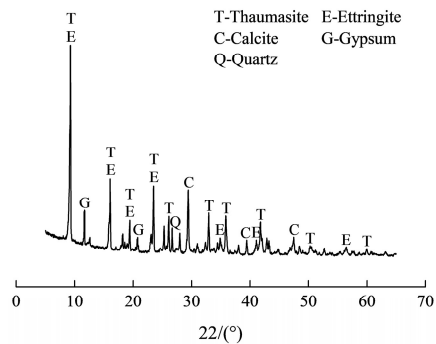


Fig. 4. XRD pattern of the soft crumbly degraded concrete

FTIR was carried out and the result was shown in Fig. 5. The wave numbers of important infrared absorption bands which was identified by comparison with previously published data shown in Table 4.

Firstly, a peak was detected at 497 cm^{-1} which was assigned to the presence of SiO_6 bonds. Si

was such an extremely rare coordinate site for mineral silicates. The presence of this peak must be indicative of either thaumasite or a thaumasite-containing solid solution. Secondly, peaks at 1390 cm^{-1} could be assigned to C-O stretching bending which attributable to the presence of the CO_3^{2-} , the peak at 1092 cm^{-1} was related to SO_4^{2-} , but there was no sign of AlO_6 at 850 cm^{-1} . The above indicated that the soft crumbly degraded concrete contained thaumasite and little ettringite. Existing research showed that thaumasite-type sulfate attack mainly occurred at the interface between lining concrete and ground, corresponded to the site investigation results.

Sulfate, silicate, carbonate, sufficient water and low temperature environment were the necessary conditions for the formation of thaumasite [6]. The ion concentration test results in Table 2 showed that sulfate content in groundwater was sufficient. The second lining concrete of the tunnel adopted Portland cement. Calcium silicon hydrate (C-S-H) that produced by hydration of Portland cement were the primary source of silicate. The main source of carbonate, forming thaumasite, not only from aggregate but also from carbonated concrete, especially carbonated concrete. In addition, due to the existence of limestone in tunnel site, the flashing of groundwater would increase the content of carbonate ions. Water leakage from lining surface and arch foot provided sufficient water for the formation of thaumasite. Existing studies shown that thaumasite was easily formed at temperatures below $15\text{ }^\circ\text{C}$, especially $0\text{-}5\text{ }^\circ\text{C}$. However, some scholars found that thaumasite could also be formed at temperatures above $15\text{ }^\circ\text{C}$, the annual average temperature in the tunnel area was about $16.4\text{ }^\circ\text{C}$. The tunnel environment created proper conditions for the formation of thaumasite. It was further confirmed that thaumasite-type sulfate attack occurred at the arch foot.

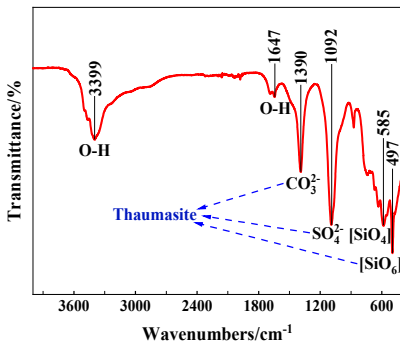


Fig. 5. FTIR spectrum of the soft crumbly degraded concrete

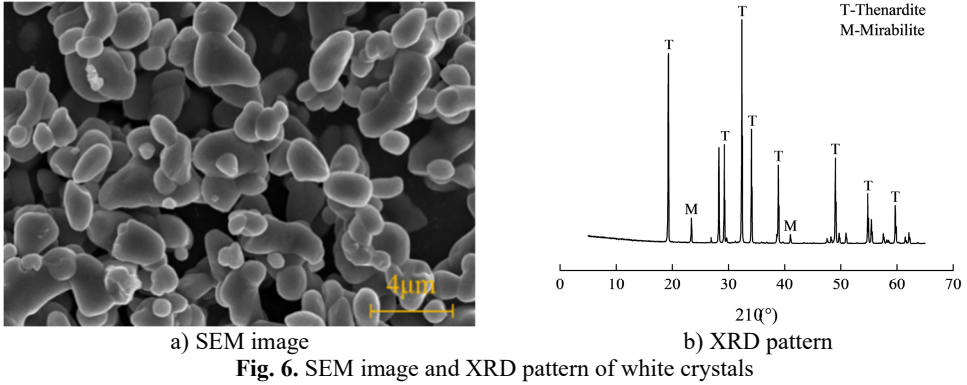
Table 4. Wave numbers of important infrared absorption bands

Wave number (cm^{-1})	Assignment
1400	CO_3^{2-} stretch
1100	SO_4^{2-} stretch
940/920	SiO_4
887	CO_3^{2-} bend
850	AlO_6
673	SiO_6 stretch
590	SiO_4 bend
500	SiO_6 bend

5.2. Drying-wetting cycle corrosion

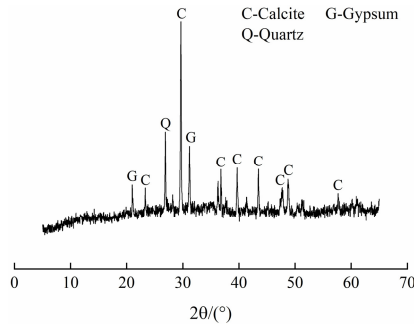
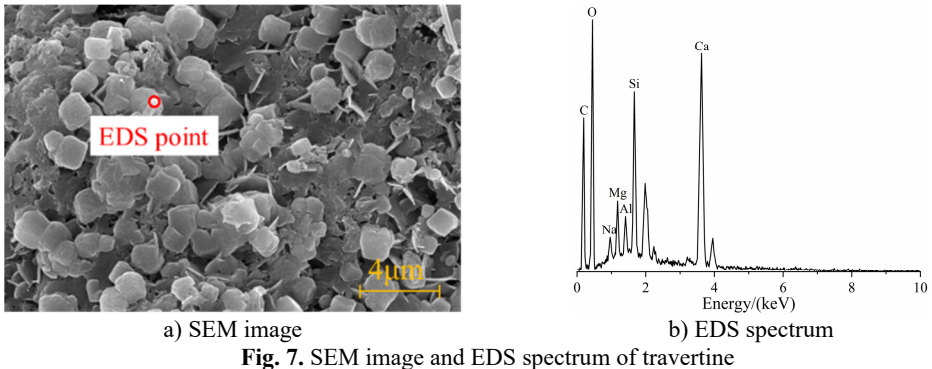
During the rainy season, the lining surface was moist. In the dry season, there was less seepage or no seepage on the secondary lining and the lining surface was relatively dry. The lining structure was in the state of soaking and drying repeatedly, which made lining concrete suffer drying-wetting cycle sulfate attack and white crystals formed on the lining surface (As 5# shown in Table 1). The SEM image and XRD pattern of white crystals were shown in Fig. 6.

From SEM image, the morphology of sodium sulfate crystal was cake-shaped with a diameter of $0.2\text{-}2\text{ }\mu\text{m}$. XRD pattern showed that the substances mainly contained sodium sulfate crystals including thenardite (Na_2SO_4) and mirabilite ($\text{Na}_2\text{SO}_4 \cdot 10\text{H}_2\text{O}$), and Na_2SO_4 was in the majority. When the crystallization pressure exceeded the tensile strength of concrete, the concrete structure would be destroyed. At different temperatures and relative humidity (RH), Na_2SO_4 and $\text{Na}_2\text{SO}_4 \cdot 10\text{H}_2\text{O}$ were interchangeable. Na_2SO_4 and $\text{Na}_2\text{SO}_4 \cdot 10\text{H}_2\text{O}$ would transform each other at about $32.4\text{ }^\circ\text{C}$. When Na_2SO_4 was converted to $\text{Na}_2\text{SO}_4 \cdot 10\text{H}_2\text{O}$, its volume increased by 315 % [7], but that didn't produce crystallization pressure. When the saturation was constant, the crystallization pressure of Na_2SO_4 was much higher than that of $\text{Na}_2\text{SO}_4 \cdot 10\text{H}_2\text{O}$.



5.3. Dissolved corrosion

The SEM image and EDS spectrum of travertine were shown in Fig. 7. From Fig. 7(a), it could be seen that these crystals had scaly shapes and were stacked upon each other. And most of calcium silicon hydrate (C-S-H) had been decomposed without obvious distribution of C-S-H gel. The result of EDS spectrum shown that the main elemental composition of travertine was Ca, Si, O and C, and also contained a small amount of Mg, Al and Na. XRD pattern of travertine was shown in Fig. 8, it showed that the main phase was calcite and also contained a small amount of gypsum and quartz, which was corresponded to the EDS result.



Under the groundwater seepage action, calcium hydroxide $[Ca(OH)_2]$ in cement stone dissolved continuously [8], which reduced the density of cement stone. HCO_3^- in groundwater reacted with $Ca(OH)_2$ and formed $CaCO_3$. When the water pressure dropped, decarbonization occurred and CO_2 escaped from water, Ca^{2+} and HCO_3^- precipitated because of $CaCO_3$ dissolving

in the surface layer, but when they were brought to the exterior of lining concrete by seepage action, CaCO_3 would form again due to the sudden drop of pressure (As 3# shown in Table 1). The dissolution and crystallization of CaCO_3 repeated again and again. When the crystallization pressure exceeded the concrete tensile strength, concrete on the lining surface would peel off.

6. Conclusions

Site investigation was carried out on a tunnel subjected to severe sulfate attack. The main conclusions were as follows:

1) The tunnel lining concrete suffered sulfate attack seriously. A large area of concrete peeled off and the soft crumbly degraded concrete appeared. There are abundant SO_4^{2-} in groundwater and the tunnel was in a medium-severe groundwater chemical corrosion environment. The actual strength grade of lining concrete didn't meet the requirements of relevant code.

2) SEM, EDS, XRD and FTIR demonstrated that the soft crumbly degraded concrete was abundant thaumasite. The formation of thaumasite made C-S-H lose its cementation ability and concrete structure lost its strength completely. The tunnel also suffered drying-wetting cycle sulfate attack with seasonal rainfall and white crystals were formed on the lining surface.

3) Besides sulfate attack, the tunnel also appeared dissolved corrosion obviously. $\text{Ca}(\text{OH})_2$ dissolved continuously due to the groundwater seepage action, which reduced the density of cement stone and decreased the concrete strength. Moreover, the dissolution and crystallization process of CaCO_3 was repeated, which would make concrete on the lining surface peel off.

Acknowledgements

The research in this paper was financially supported by the Mechanical Effect and Safety Analysis of Severely Damaged Tunnel Renovation Process (Grant No. H20210058).

References

- [1] M. Lei, L. Peng, C. Shi, and S. Wang, "Experimental study on the damage mechanism of tunnel structure suffering from sulfate attack," *Tunnelling and Underground Space Technology*, Vol. 36, No. 2, pp. 5–13, Jun. 2013, <https://doi.org/10.1016/j.tust.2013.01.007>
- [2] B. Ma, X. Gao, E. A. Byars, and Q. Zhou, "Thaumasite formation in a tunnel of Bapanxia dam in Western China," *Cement and Concrete Research*, Vol. 36, No. 4, pp. 716–722, Apr. 2006, <https://doi.org/10.1016/j.cemconres.2005.10.011>
- [3] K.-L. Ma, G.-C. Long, and Y.-J. Xie, "Railway tunnel concrete lining damaged by formation of gypsum, thaumasite and sulfate crystallization products in southwest of China," *Journal of Central South University*, Vol. 19, No. 8, pp. 2340–2347, Aug. 2012, <https://doi.org/10.1007/s11771-012-1280-2>
- [4] R. Yin, C. Zhang, Q. Wu, B. Li, and H. Xie, "Damage on lining concrete in highway tunnels under combined sulfate and chloride attack," *Frontiers of Structural and Civil Engineering*, Vol. 12, No. 3, pp. 331–340, Sep. 2018, <https://doi.org/10.1007/s11709-017-0421-y>
- [5] S. J. Barnett, D. E. Macphee, E. E. Lachowski, and N. J. Crammond, "XRD, EDX and IR analysis of solid solutions between thaumasite and ettringite," *Cement and Concrete Research*, Vol. 32, No. 5, pp. 719–730, May 2002, [https://doi.org/10.1016/s0008-8846\(01\)00750-5](https://doi.org/10.1016/s0008-8846(01)00750-5)
- [6] Z. Liu, D. Deng, G. de Schutter, and Z. Yu, "The effect of MgSO_4 on thaumasite formation," *Cement and Concrete Composites*, Vol. 35, No. 1, pp. 102–108, Jan. 2013, <https://doi.org/10.1016/j.cemconcomp.2012.08.011>
- [7] S. R. Liu, J. J. Yang, Z. Z. Wang, H. Rong, and L. Zhang, "Self-healing Performance of Concrete in Sodium Sulfate Solution," *Journal of the Chinese Ceramic Society*, Vol. 43, No. 8, pp. 1083–1089, 2015, <https://doi.org/10.14062/j.issn.0454-5648.2015.08.10>
- [8] J. H. Liu, L. B. Bian, W. He, H. G. Ji, W. J. Zhou, and C. W. Han, "Investigation and destruction mechanism on corrosion of concrete shaft in coal mine," *Journal of China Coal Society*, Vol. 40, No. 3, pp. 528–533, 2015, <https://doi.org/10.13225/j.cnki.jccs.2014.0585>